JOURNAL OF
Materials
CHEMISTRY

# Mechanism of sensing CO in nitrogen by nanocrystalline $SnO_2$ and $SnO_2$(Pd) studied by Mössbauer spectroscopy and conductance measurements

**Olga Safonova, Igor Bezverkhy, Pavel Fabrichnyi, Marina Rumyantseva and Alexandre Gaskov***

*Chemistry Department, Moscow State University, Leninskie Gory, Moscow 119899, Russia.*
*Tel: +7 095 9395471; Fax: +7 095 9390998; E-mail: gaskov@inorg.chem.msu.ru*

***Received 10th October 2001, Accepted 19th December 2001***
***First published as an Advance Article on the web 7th February 2002***

The mechanism of CO/$N_2$ sensitivity of undoped and Pd-doped nanocrystalline tin dioxide was studied *in situ* by coupled electrical measurements and $^{119}$Sn Mössbauer spectroscopy. Nanocrystalline $SnO_2$ with a grain size of about 6–8 nm was synthesized by the sol–gel method. $SnO_2$(Pd) ([Pd] = 1 at%) was prepared from $SnO_2$ by the impregnation method. Electrical properties of $SnO_2$ and $SnO_2$(Pd) in the presence of CO/$N_2$ were studied at a fixed temperature in the range $50 \leqslant T \leqslant 380$ °C. Addition of Pd strongly increases the sensor response to CO over the whole temperature range. It was shown by Mössbauer spectroscopy that two different mechanisms of gas sensitivity can exist in the presence of CO/$N_2$. The first "low temperature" mechanism ($T < 100$ °C) may be attributed to redox reactions between surface oxygen and CO catalyzed by $PdO_x$ clusters. The second "high temperature" one (125–380 °C) involves oxygen vacancies diffusing into the bulk of the tin dioxide grains which leads to reversible reduction of Sn(IV) to Sn(II).

## Introduction

Nanocrystalline $SnO_2$ films and ceramics are widely used as solid-state gas sensors that can change their electrical properties during interaction with gas molecules.[1] Nevertheless the mechanism of the sensing effect in the majority of cases is still under discussion. Tin dioxide is a wide band gap n-type semiconductor. For $SnO_2$ single crystals, the electron concentration depends on stoichiometry deviation determined by oxygen vacancies ($V_O$), which are predominant atomic defects.[2] The electrical properties of nanocrystalline $SnO_2$ depend strongly on surface states which are produced by oxygen and other gas molecules chemisorbed at the grain boundaries and which results in space charge appearance and band modulation.[1,3] Therefore, the variation of the chemisorbed molecule density is supposed to be the main factor responsible for the electrical response, whereas the tin dioxide phase remains chemically stable. Dopant metals such as Pt, Pd or Ag form metallic clusters on the surface of $SnO_2$ grains, produce additional adsorption sites and may catalyse redox reactions on the surface. However, studies[1,3–6] of polycrystalline tin dioxide interactions with reducing gases, carried out by different surface analysis techniques, suggest a more complicated mechanism which includes the removal of lattice oxygen, modification of the oxidation state of tin, and creation of new bonds between native and dopant metals. At the same time, it appears very difficult to investigate such processes in nanocrystalline systems. Since chemical reactions with gases can proceed very rapidly, characterization of nanocrystalline oxides are to be performed *in situ*, *i.e.* in the reaction atmosphere. High vacuum and high energy treatments are obligatory in conventional surface analysis techniques such as AES and XPS and induce changes in the surface state, which limit the application of these methods. *In situ* FTIR, Raman, EPR, EXAFS and XANES spectroscopies are considered to be the most promising methods. Detailed studies[7] of the interaction of $SnO_2$(Pt) with CO/$N_2$ by *in situ* coupled XANES and electrical conductance measurements indicate that modification of the oxidation state of $PtO_x$ clusters proceeds synchronously with the electrical response. A similar mechanism is predicted for Pd in $SnO_2$(Pd). Nevertheless the role of the tin dioxide matrix in a gas sensor response is still unclear. *In situ* EPR measurements[8] confirm the change of chemisorbed oxygen $O_2{}^-{}_S$ and single ionized oxygen vacancy $V^{\bullet}{}_O$ concentration in $SnO_2$ during interaction with CO/$N_2$ gas mixtures, but this method could not determine the tin oxidation state. This problem can be solved by Mössbauer spectroscopy. Thus, in this work we tried to clarify the role of the tin dioxide matrix and palladium additive in CO-response of nanocrystalline tin dioxide-based materials by coupled *in situ* conductivity measurements and $^{119}$Sn Mössbauer spectroscopy. As Sn(II) ions have proven to be unstable and easily oxidizable, *in situ* Mössbauer characterisation of the valence state of tin therefore becomes of particularly important concern.

## Experimental

Tin dioxide nanocrystalline powder was prepared by conventional hydrolysis of $SnCl_4$. A measured amount of $SnCl_4 \cdot 5H_2O$ was dissolved in deionized water in an ice bath and liquid ammonia was slowly added to the stirred solution to achieve complete precipitation of α-stannic acid. The resulting gel was centrifuged and washed with deionized water until no chloride ion remained ($AgNO_3$ test). The precipitate was dried at 100 °C overnight and ground in an agate mortar. Then the samples of $SnO_2$ powder were calcinated at 300 °C for 24 h. The X-ray powder diffraction confirms the nanocrystalline state of tin dioxide.

$SnO_2$(Pd) ([Pd] = 1 at%) powder was obtained by the impregnation method. A measured amount of 0.05 M palladium acetylacetonate solution in acetic acid was added to previously prepared $SnO_2$ powder. The mixture was dried at room temperature for 24 h and then calcinated at 300 °C for 24 h for full evaporation of acetic acid, and palladium acetylacetonate decomposition.

DOI: 10.1039/b109219g

**This journal is © The Royal Society of Chemistry 2002**

For electrical measurements thick films of $SnO_2$ and $SnO_2$(Pd) were prepared by the screen printing technique. $SnO_2$ and $SnO_2$(Pd) powders calcinated at 300 °C were mixed with binder (terpineol (α,α,4-trimethylcyclohex-3-ene-1-methanol)-ethyl cellulose–ethanol mixture) and deposited on polycrystalline $Al_2O_3$ substrates with golden contacts prepared by the thermal evaporation method (Au 0.9999%). Then films were dried at 100 °C for 24 h and calcinated at 500 °C for 6 h. The area of the films was 7 mm × 2 mm.

The X-ray diffraction (XRD) patterns were recorded using a STOE diffractometer with monochromatic Cu ($K_\alpha$) radiation. The results were processed with use of STOE Win XPow software. Crystallite sizes, *d*, were determined from the Debye–Scherrer equation.

For *in situ* kinetic characterization of the oxidation state of tin simultaneously with conductivity measurements a special reactor equipped with a thin-wall Mössbauer sample-cell and an electric conductance measurement system was utilized. $^{119}$Sn Mössbauer spectra were recorded using powder samples whereas conductance measurements were performed on relevant thick films. Before every experiment a measured amount of tin dioxide powder and the corresponding film were heated in the reactor at a fixed temperature of 380 °C in a dry air flow for 2 h to obtain a reproducible state of the material.

Measurements of electric current proportional to the conductance value were performed in dc mode at the fixed voltage $U = 1$ V. The kinetics of conductance change of a film under exposure to an atmosphere of 1% CO in $N_2$ were measured at fixed operating temperatures in the range $50 \leqslant T \leqslant 380$ °C. Certified 1 ± 0.02% CO/$N_2$ ($O_2$ < 20 ppm, $H_2O$ < 3 ppm) gas mixtures have been used. The gas flow rate varied from 0.25 to 10 l h$^{-1}$.

Prior to Mössbauer measurements powders were exposed to a flux of 1% CO/$N_2$ gas mixture in the reactor at a fixed temperature in the range $50 \leqslant T \leqslant 380$ °C during a fixed period of time *t*, rapidly cooled in the same gas atmosphere down to room temperature, and *in situ* transferred into the sample-cell. $^{119}$Sn spectra were recorded at 100 K using a conventional spectrometer operating in constant acceleration mode with a Ca$^{119m}$SnO$_3$ source. Isomer shift values refer to a $CaSnO_3$ absorber at 298 K.

## Results and discussion

### Composition and microstructure

XRD data demonstrate that both $SnO_2$ and $SnO_2$(Pd) samples were of the casseterite $SnO_2$ structure. No palladium containing phases have been detected apparently owing to both the low content and the small dimensions of their clusters. The average size *d* of $SnO_2$ crystallites calculated from X-ray diffraction patterns using the Debye–Scherrer equation are found to vary from 6 to 8 nm for as synthesised $SnO_2$ and $SnO_2$(Pd) powders. After all the experiments at elevated temperatures (annealing in CO and air for Mössbauer measurements) the grain size became slightly higher but did not exceed 10 nm.

### Electrical properties of the films in the presence of CO

Fig. 1 shows the electrical response of $SnO_2$ (a) and $SnO_2$(Pd) (b) films to periodical changes of gas atmosphere from dry air to 1% CO in $N_2$ at 50, 100, 200, and 380 °C. The gas flow rate was 10 l h$^{-1}$; it was verified that under these conditions the kinetics of conductance change were independent of the flow rate and limited only by the rate of the solid–gas interaction. The main features of the observed transients may be summarised as follows: (i) Pd doping significantly affects the sensitivity to CO. $SnO_2$(Pd) films exhibit a rapid and pronounced increase in electrical conductance with the adsorption of CO even at 100 °C. Sensitivity of this film is higher by several orders than that for a pure $SnO_2$ film. (ii) The maximum conductance value for $SnO_2$(Pd) film under exposure to CO is close to the conductance of $SnO_2$ film under the same conditions. Hence, it appears that the interaction with CO suppresses the effect of the Pd dopant on the electric properties of the films. The data presented allow us to suggest the existence of two different mechanisms of conductance response.

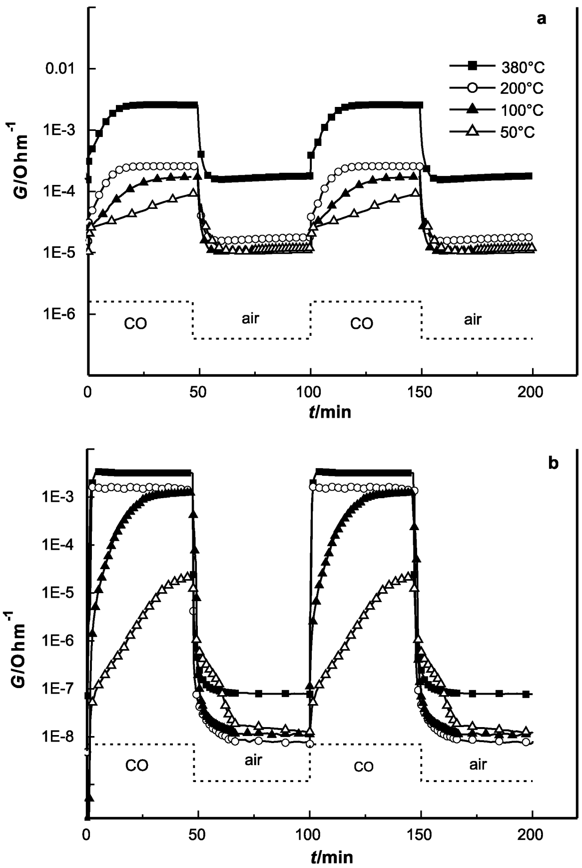

**Fig. 1** The electrical response of $SnO_2$ (a) and $SnO_2$(Pd) (b) films with periodical changes of gas atmosphere from dry air to 1% CO/$N_2$ at 50, 100, 200, and 380 °C.

It was shown earlier[9] that a decrease of gas flow rate significantly affects the conductance response of $SnO_2$(Pd). Electrical responses of the $SnO_2$(Pd) film measured under a low gas flow rate (0.25–4 l h$^{-1}$) of 1% CO/$N_2$ gas mixture at 380 °C (a) and 100 °C (b) are shown in Fig. 2. At 380 °C the change in the kinetics of conductance is complicated and depends on the rate of gas flux in the reactor. Two stages of conductance increase in the *G*(*t*) curves are clearly observed (Fig. 2a); the first just after exposure to CO, and the second after a period of induction. On the contrary, at 100 °C (Fig. 2b) the rate of conductance change decreases monotonously with the decrease of the rate of CO flux while the shape of the curves remains essentially the same. Similar *G*(*t*) dependencies at 380 °C were observed earlier for pure $SnO_2$ films doped with Pt, Ni, Cu.[9] Thus, these kinetic features are to be related to tin dioxide matrix transformations and can not be explained only by the presence of palladium.

### *In situ* Mössbauer spectroscopy combined with conductance measurements

The effect of exposure to CO on the oxidation state of tin in $SnO_2$ and $SnO_2$(Pd) materials under different conditions was studied. The variable parameters were temperature, time of exposure, and gas flow rate.

Fig. 3 shows the Mössbauer spectra of $SnO_2$(Pd) in air and after 60 min exposure to a 1% CO/$N_2$ gas mixture under 4 l h$^{-1}$

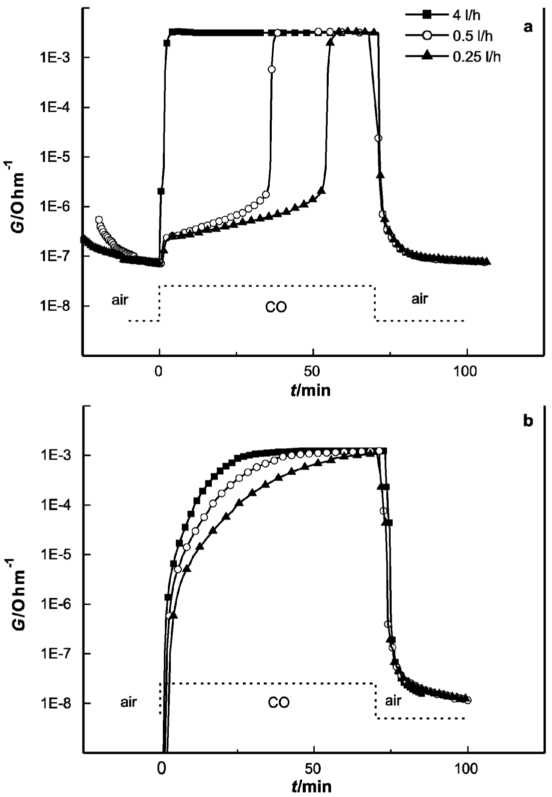

**Fig. 2** Electrical response of $SnO_2(Pd)$ film in 1% CO + $N_2$ at 380 °C (a) and 100 °C (b) at 4 l $h^{-1}$, 0.5 l $h^{-1}$, and 0.25 l $h^{-1}$ gas flow rates.

flow rate at 380 °C. Parameters of the predominant spectral component ($\delta = 0.00 \pm 0.02$ mm $s^{-1}$, $\Delta = 1.2 \pm 0.02$ mm $s^{-1}$) associated with Sn(IV) within the accuracy of the measurements are those of the $^{119}$Sn(IV) in the reference sample of crystalline $SnO_2$. Thus, the nanocrystalline state of the oxide studied does not noticeably affect the value of the electron density at $^{119}$Sn nuclei. Under exposure to CO the contribution of the Sn(II) doublet is clearly observed in the spectrum. Similar experiments with pure $SnO_2$ have also shown the appearance of an Sn(II) doublet after 60 min interaction with CO. The observed values of isomer shift $\delta = 2.74 \pm 0.04$ mm $s^{-1}$ and quadruple splitting $\Delta = 1.93 \pm 0.04$ mm $s^{-1}$ point to the presence of a stereochemically active lone pair[10] and are similar to those of Sn(II) ions on low coordination sites on the surface of $Cr_2O_3$, $V_2O_3$ and $\alpha$-$Al_2O_3$ matrix crystallites.[11] No metallic tin was detected in these spectra as well as in those obtained in further experiments at 25, 100, 125, 150 and 250 °C. In addition, the behaviour of crystalline $SnO_2$ ($d$ >500 nm) as a reference material was studied under the same conditions (Fig. 4). Sn(II) molar concentrations were calculated on the basis of the known tin content in the tin dioxide sample introduced into the measurement cell and the normalised Sn(II) absorption areas observed in the spectra after exposure to CO. The absorption areas at 100 K for this purpose were converted, in the thin absorber approximation, to the number of Sn(II) per cm$^2$, assuming the recoilless fraction $f' = 0.75$ (average value for Sn(II) ions located on surface sites according to the Mössbauer lattice temperature values $\Theta_M$ reported in ref. 11).

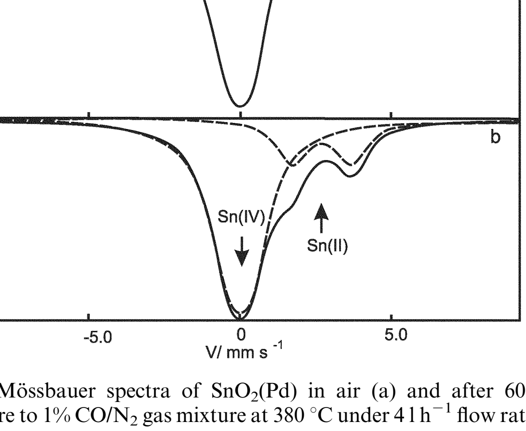

**Fig. 3** Mössbauer spectra of $SnO_2(Pd)$ in air (a) and after 60 min exposure to 1% $CO/N_2$ gas mixture at 380 °C under 4 l $h^{-1}$ flow rate (b).

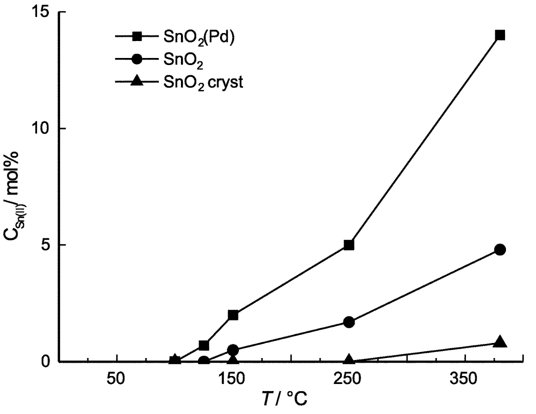

**Fig. 4** Concentration of Sn(II) in nanocrystalline $SnO_2$, nanocrystalline $SnO_2(Pd)$ and crystalline $SnO_2$ after 60 min exposure to 1% $CO/N_2$ at different temperatures.

The data presented in Fig. 5 allows the following points to be noted: (i) exposure of nanocrystalline $SnO_2$ and $SnO_2(Pd)$ to a 1% $CO/N_2$ gas mixture results in the appearance of Sn(II) at temperatures higher than 125 °C. (ii) Pd catalyses tin dioxide reduction as demonstrated by the increase in Sn(II) concentration. (iii) The reactivity of crystalline $SnO_2$ is much lower compared with that of tin dioxide in the nanocrystalline state. Thus, in the low temperature region $T$ < 100 °C the observed electrical response can not be assigned to tin dioxide reduction

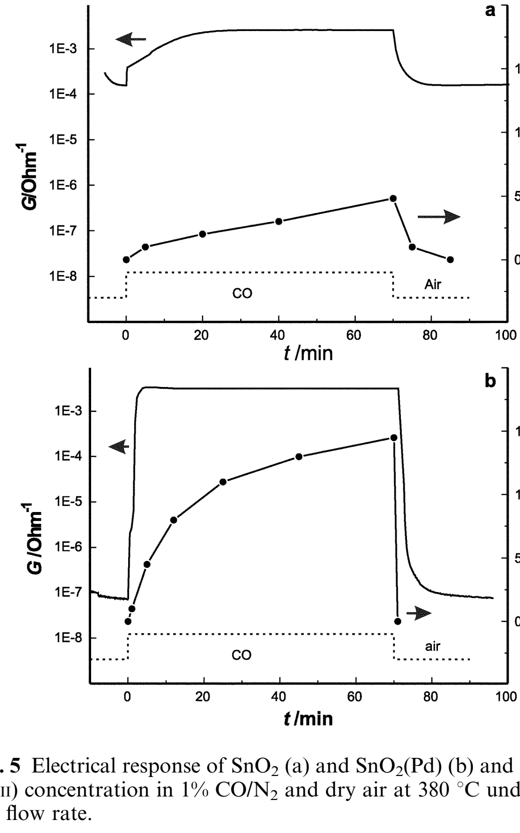

**Fig. 5** Electrical response of $SnO_2$ (a) and $SnO_2(Pd)$ (b) and change of Sn(II) concentration in 1% $CO/N_2$ and dry air at 380 °C under 4 l $h^{-1}$ gas flow rate.

and most probably results from interaction of CO with surface oxygen species and parallel reduction of palladium clusters in the case of $SnO_2$(Pd). This mechanism can be defined as the "low-temperature" one. At higher temperatures (125–380 °C), the conductance increase under exposure to CO can be accounted for by the reduction of tin dioxide. These data are in agreement with *in situ* EPR measurement.[8]

Further experiments concerned this "high temperature" mechanism and were performed at 380 °C. Fig. 5 shows the electrical response combined with a change of Sn(II) concentration revealed by *in situ* Mössbauer spectra for nanocrystalline $SnO_2$ and $SnO_2$(Pd) in the presence of CO and dry air at 380 °C. The gas flow rate was fixed at 4 l $h^{-1}$. Mössbauer spectra of $SnO_2$(Pd) exposed to CO atmosphere and then to dry air are shown in Fig. 6. It can be seen that the conductance change under gas atmosphere cycling occurs simultaneously with the change of the tin oxidation state. A rapid and pronounced increase in Sn(II) spectral contribution is observed just after CO admission into the reactor. The Sn(II) component disappears 1 min after air admission. Two interesting points should be noted. Firstly, it appears that a very low Sn(II) content ($<1$ mol%) is sufficient for the conductance to change by 1000 times. Secondly, a further increase of Sn(II) concentration up to 14 mol% under exposure to CO does not significantly change the conductance value.

Fig. 7 shows the electrical response combined with the change of Sn(II) concentration revealed by *in situ* Mössbauer spectra for nanocrystalline $SnO_2$(Pd) when gas flow rate was fixed at 0.5 l $h^{-1}$ (a) and 0.25 l $h^{-1}$ (b). The first stage of conductance growth observed on $G(t)$ curves for $SnO_2$(Pd) proves not to be associated with tin dioxide matrix reduction. On the contrary, the second stage, which just precedes Sn(II) appearance in Mössbauer spectra, can display earlier steps of $SnO_2$ surface reduction.

On the basis of the results obtained the following model of tin dioxide interaction with CO can be proposed. The mechanism of CO gas sensitivity of nanocrystalline $SnO_2$ seems to be temperature-dependent. At low temperatures ($T <$ 100 °C) surface oxygen species may react with CO to produce a large amount of oxygen vacancies at the $SnO_2$ grain surface *via* the following reactions:

$$O_O^{\times} = O^{2-}{}_S + V^{\bullet\bullet}{}_O \qquad (1)$$

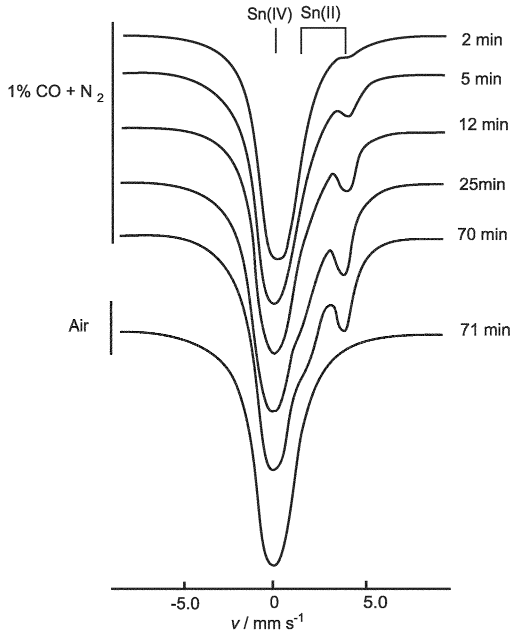

**Fig. 6** Mössbauer spectra of $SnO_2$(Pd) in a 1% $CO/N_2$ atmosphere and then in dry air at 380 °C.

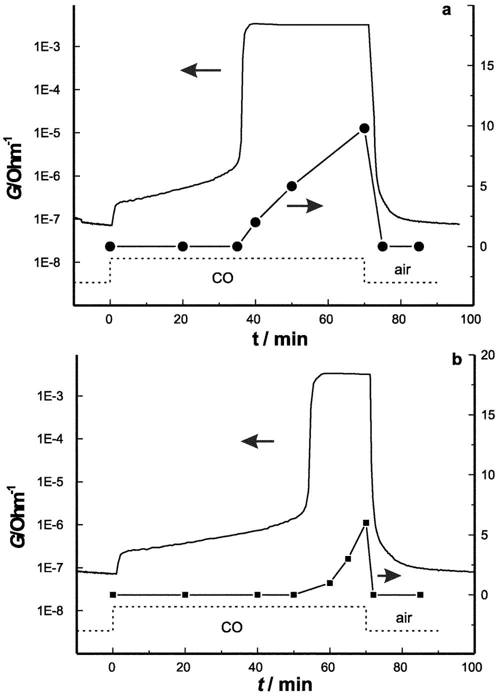

**Fig. 7** Electrical response of $SnO_2$(Pd) and change of Sn(II) concentration in 1% $CO/N_2$ and dry air at 380 °C under 0.5 l $h^{-1}$ (a) and 0.25 l $h^{-1}$ (b) gas flow rates.

$$O^{2-}{}_S + CO = CO_2 + 2e \qquad (2)$$

$$O_2^{-}{}_S + 2CO = 2CO_2 + e \qquad (3)$$

This results in both an increase in electron concentration and a decrease in the height of the electron barriers at the surface of tin dioxide grains. The reaction kinetics are limited at low temperatures by the oxygen diffusion between the regular anion positions in $SnO_2$ and the grain surface.

$PdO_x$ clusters may catalyse these surface reactions by the following processes:

$$PdO + CO = Pd + CO_2 \qquad (4)$$

$$Pd + O^{2-}{}_S = PdO + 2e \qquad (5)$$

thus enhancing the electrical response.

At higher temperatures oxygen diffusion between surface and volume regions of tin dioxide grains becomes large enough to affect the concentration of surface oxygen vacancies in nanocrystalline $SnO_2$ (eqn. (1)). Under such conditions conductance changes rapidly by several orders of magnitude only when composition of tin dioxide grains attain the limit of the stability region corresponding to the maximum oxygen deficit. This process is to be related to earlier steps of $SnO_2$ surface reduction. It was shown[12] that SnO is a narrow gap semiconductor $E_g = 0.4$ eV (300 K). Hence when dispersed on the surface of $SnO_2$ grains it can give rise to significant electrical conductance growth.

## Conclusions

Nanocrystalline $SnO_2$ and $SnO_2$(Pd) ([Pd] = 1 at%) powders and thick films with grain size of about 6–8 nm were synthesized by the sol–gel method.

The mechanism of $CO/N_2$ sensitivity in the materials obtained was studied *in situ* by coupled electrical measurements and $^{119}Sn$ Mössbauer spectroscopy. It was shown that the electrical response of both $SnO_2$ and $SnO_2$(Pd) at 125–380 °C is associated with the process announcing the beginning of the

Sn(IV) to Sn(II) transition. No metallic tin was detected in the spectra.

## Acknowledgement

This work was supported by INTAS grant 2000-0066 and RFBR grant 01-03-32728.

## References

1 W. Gopel and K. Schierbaum, *Sens. Actuators, B*, 1995, **26–27**, 1.
2 C. G. Fonstadt and R. H. Rediker, *J. Appl. Phys.*, 1971, **42**, 2911.
3 S. Chang, *J. Vac. Sci. Technol.*, 1980, **17**, 366.
4 P. Romppainen and V. Lantto, *J. Appl. Phys.*, 1988, **63**, 5159.
5 M. W. Prins, K.-O. Grosse-Holz, J. F. M. Cillessen and L. F. Feiner, *J. Appl. Phys.*, 1998, **83**, 888.
6 S. D. Gardner, G. B. Hoflund and D. R. Schryer, *J. Catal.*, 1989, **119**, 179.
7 M. Gaidi, J. L. Hazemann, I. Matko, B. Chenevier, M. Rumyantseva, A. Gaskov and M. Labeau, *J. Electrochem. Soc.*, 2000, **147**, 3131.
8 C. Canevali, N. Chiodini, P. Di Nola, F. Marazzoni, R. Scotti and C. L. Bianchi, *J. Mater. Chem.*, 1997, **7**, 997.
9 O. V. Safonova, M. N. Rumyantseva, R. I. Kozlov, M. Labeau, G. Delabouglise, L. I. Ryabova and A. M. Gaskov, *Mater. Sci. Eng., B*, 2000, **77**, 159.
10 A. J. F. Boyle, B. S. P. Bunbury and C. Edwards, *Proc. Phys. Soc., London*, 1962, **79**, 416.
11 M. I. Afanasov and P. B. Fabritchnyi, *Ross. Khim. Zh.*, 1996, **50**, 54.
12 B. P. Kryzhanovsky and A. Ya. Kuznetsov, *Russ. J. Phys. Chem. (Transl. of Zh. Fiz. Khim.)*, 1961, **35**, 80.